Chapter 24

Use of Resonance Energy Transfer Techniques for In Vivo Detection of Chemokine Receptor Oligomerization

Laura Martínez-Muñoz, José Miguel Rodríguez-Frade, and Mario Mellado

Abstract

Since the first reports on chemokine function, much information has been generated on the implications of these molecules in numerous physiological and pathological processes, as well as on the signaling events activated through their binding to receptors. As is the case for other G protein-coupled receptors, chemokine receptors are not isolated entities that are activated following ligand binding; rather, they are found as dimers and/or higher order oligomers at the cell surface, even in the absence of ligands. These complexes form platforms that can be modified by receptor expression and ligand levels, indicating that they are dynamic structures. The analysis of the conformations adopted by these receptors at the membrane and their dynamics is thus crucial for a complete understanding of the function of the chemokines. We focus here on the methodology insights of new techniques, such as those based on resonance energy transfer for the analysis of chemokine receptor conformations in living cells.

Key words Chemokines, GPCR, Oligomerization, FRET, BRET, BiFC, SRET

1 Introduction

1.1 Chemokines and Their Receptors: A Dynamic System

Chemokines are a family of structurally related, low-molecular-weight pro-inflammatory cytokines involved in recruitment of specific cell populations to target tissues by interacting with members of the G protein-coupled receptor (GPCR) family [1–4]. Although originally described as specific mediators of leukocyte directional movement, they are now implicated in a much wider variety of physiological and pathological processes including tumor cell growth and metastasis, atherosclerosis, angiogenesis, chronic inflammatory disease, and HIV-1 infection [2, 5–10].

In man, more than 50 chemokines and 20 receptors have been described and classified according to functional criteria as pro-inflammatory or homeostatic chemokines, depending on their role in inflammation or in immune system homeostasis, respectively [1, 11]. Although chemokines and their receptors were once considered

Tian Jin and Dale Hereld (eds.), *Chemotaxis: Methods and Protocols*, Methods in Molecular Biology, vol. 1407,
DOI 10.1007/978-1-4939-3480-5_24,

independent, isolated entities, the situation is much more complex than initially anticipated. Chemokines can form dimers, tetramers, and even oligomers [12, 13]. They interact not only with chemokine receptors but can also bind cell surface glycosaminoglycans as well as non-signaling scavenger receptors [1, 14, 15]. Chemokine receptors interact with chemokines and also other molecules, such as defensins and virally encoded chemokines [2, 16–19].

Whereas some data indicate that GPCR family members can function as monomers [20], increasing experimental evidence indicates that these receptors form homodimeric and heterodimeric complexes at the cell membrane [21–25] not only with other chemokine receptors, but also with other GPCR (e.g., EBI2, delta opioid receptor) [26, 27] and other membrane proteins (e.g., CD4, CD26, T cell receptor, tetraspanins) [28–32]. These receptor complexes are functional entities that mediate biological responses and are associated with modulation of ligand binding and of G protein associations, and with activation of signaling events distinct from those triggered by individual receptors [33, 34]. Heterodimerization is the mechanism that underlies delayed AIDS progression in HIV-1-infected patients bearing the CCR2V64I polymorphism [35]; CCR5 expression alters CD4/CXCR4 heterodimer conformation, thus blocking M-tropic HIV-1 binding and infection [28]. Heterodimers activate specific signaling cascades that differ from those activated by homodimers [33, 36]. In contrast to homodimer-triggered Gi signaling, CCR2/CCR5 heterodimers activate G_{11}, which alters PI3K induction kinetics [33]. CCR5 and CXCR4 heterodimerization with opioid receptors modulates chemokine responses [27, 37, 38]. Oligomeric complexes can also regulate ligand affinity; for example, CXCR5 and EBI2 heterodimers reduce CXCL13 affinity for CXCR5, as well as subsequent Gi protein activation [26]. In this scenario, chemokine-mediated signaling properties depend on the receptor complex stabilized. This defines a very dynamic universe that offers ample possibilities for regulating chemokine function, and allows the design of innovative drugs to target specific chemokine-mediated functions without altering others.

Although biochemical approaches were initially used to determine chemokine receptor expression at the cell membrane as well as the signaling molecules involved in chemokine function, they render a static view of the system that can lead to misinterpretation of results. For example, western blot and coimmunoprecipitation showed CCR2 dimers only after ligand activation, which led us to describe an active role for ligands in receptor dimerization [23, 39]. Later studies using imaging-based techniques showed that dimers form in the absence of chemokines [21, 40, 41]. Our initial conclusion was thus incorrect; the difficulty in detecting these complexes by immunoprecipitation might be due to dimer conformational instability in the absence of ligand.

1.2 Resonance Energy Transfer Technology

Newer methods now in wide use for evaluating chemokine receptor oligomerization in living cells are based on resonance energy transfer (RET). These techniques are also useful for determining conformation dynamics, identifying the role of ligands and/or receptors in this process, and defining the dimerization site in the cell [42].

RET measurement allows identification of molecular interactions using techniques based on the quantitative theory developed by Förster in the 1940s. RET is a non-radioactive quantum mechanical process that neither requires electron collision nor involves heat production. There are two main types of RET, fluorescence resonance energy transfer (FRET) and bioluminescence resonance energy transfer (BRET); in the former, the donor fluorochrome transfers energy to an acceptor fluorochrome and in the latter, the donor molecule is luminescent [43, 44].

Both methods require generation of fusion proteins between the receptor and the fluorescent/luminescent donor and acceptor proteins, as well as the use of transfected cells [45]. Although BRET has been used for single-cell analysis [46], it is a more appropriate approach for cell suspensions [47]. It allows measurement of energy transfer between receptors, independently of their expression pattern. Dimers at the plasma membrane cannot be distinguished from those being synthesized or trafficking through the endoplasmic reticulum. BRET saturation curves can nonetheless be quantitated, as reported for CCR5/CCR2 heterodimers [48] and CXCR4 homodimers [40]. In contrast, FRET imaging using confocal microscopy allows measurements in single cells and identification of specific cell locations. FRET requires robust controls to discard direct acceptor activation by the light used to excite the donor, to eliminate nonspecific random collisions, and to monitor receptor overexpression [49].

2 Materials

2.1 Materials Common to all Techniques Described

1. HEK-293T cells (ATCC® CRL-11268™, Manassas, VA) (*see* **Note 1**).
2. DMEM culture medium containing 10 % fetal calf serum, 1 mM sodium pyruvate, and 2 mM l-glutamine (complete DMEM).
3. Tissue culture 6-well plates.
4. Cell incubator with 5%CO_2.
5. Polyethylenimine (PEI, Sigma-Aldrich, St Louis, MO).
6. 150 mM NaCl.
7. Hank's balanced salt solution (HBSS) supplemented with 0.1 % glucose.

Table 1
Combinations of fluorescent protein fragments for BiFC

Fusion[a]	Purpose	Excitation filter(s) (nm)	Emission filter(s) (nm)
A-YN155 B-YC155	A–B interaction	480–520	495–565
A-YN173 B-YC173	A–B interaction	480–520	495–565
A-CN155 B-CC155	A–B interaction	426–446	440–500
A-YN155 B-CN155 Z-CC155	Simultaneous visualization of A and B interaction with Z	480–520 and 426–446	505–565 and 440–500

[a]YN155 corresponds to EYFP residues 1–154, YC155 to EYFP 155–238, YN173 to EYFP 1–172, YC173 to EYFP 173–238, CN155 to ECFP 1–154, and CC155 to ECFP 155–238 (Table adapted from Kerppola [56])

8. Bradford protein assay (Bio-Rad, Hercules, CA).
9. Black 96-well microplates (OptiPlate, PerkinElmer, Waltham, MA).
10. Multilabel fluorescent plate reader (EnVision, Perkin Elmer).
11. Statistical analysis software (GraphPad PRISM, GraphPad Software Inc., San Diego, CA and MATLAB, The Mathworks Inc., Natick, MA).

2.2 Additional Material for BRET, BRET-BiFC, and SRET Analysis

1. Flat-bottom white 96-well microplates (Corning 3912, Corning, NY).
2. Coelenterazine H (p.j.k GmbH, Germany).
3. DeepBlueC (Biotium Inc., Hayward, CA).

2.3 Expression Vectors for Fluorescent and Luminescent Proteins

1. pECFP-N1, pEYFP-N1, pEdsRed-N1 (Clontech, Mountain View, CA) (*see* **Notes 2** and **3**).
2. For BRET assays use C-terminal part of the chemokine receptor fused to the *Renilla* luciferase gene using the pRLuc-N1 plasmid (PerkinElmer).
3. For BiFC assays, use N- and C-terminal nonfluorescent fragments of a specific fluorescent protein (*see* Table 1) cloned in pcDNA3.1 (Addgene, Cambridge, MA) (*see* **Note 4**).

3 Methods

3.1 Fluorescence Resonance Energy Transfer

The FRET mechanism involves a donor fluorophore in an electron-excited state that can transfer its excitation energy to a nearby acceptor chromophore in a non-radioactive fashion through

Table 2
Properties of fluorescent protein pairs for FRET

Fluorescence protein pair	Donor excitation maximum (nm)	Acceptor emission maximum (nm)	Donor quantum yield	Förster distance (nm)
EBFP2–mEGFP	383	507	0.56	4.8
ECFP–EYFP	440	527	0.40	4.9
Cerulean–Venus	440	528	0.62	5.4
MICy–mKO	472	559	0.90	5.3
TFP1–mVenus	492	528	0.85	5.1
CyPet–YPet	477	530	0.51	5.1
EGFP–mCherry	507	510	0.60	5.1
Venus–mCherry	528	610	0.57	5.7
Venus–tdTomato	528	581	0.57	5.9
Venus–mPlum	528	649	0.57	5.2

long-range dipole–dipole interactions. This phenomenon is not mediated by photon emission and in many applications, energy transfer results in quenching of donor fluorescence and subsequent reduction of fluorescence lifetime; this process is obviously also accompanied by an increase in acceptor fluorescence emission. The range over which energy transfer can take place is limited to approximately 10 nm (100 Å), a sufficient distance to consider that molecular interactions take place. FRET efficiency is thus extremely sensitive to the distance between donor and acceptor.

Although there are many fluorescent proteins pairs used as FRET donor/acceptors (Table 2), they respond to several common requirements.

1. The donor emission spectrum must overlap the acceptor excitation spectrum. If there is donor–acceptor interaction, donor excitation with the maximum absorbance wavelength must increase the intensity of the maximum emission fluorescence of the acceptor.
2. Energy transfer efficiency depends on the relative orientations of the donor emission dipole and the acceptor absorption dipole.
3. Donor and acceptor molecules must be located within 1–10 nm of one another. Energy transfer efficiency between donor and acceptor molecules decreases as the sixth power of the distance between the two fluorescent molecules as described by the Förster equation:

$$E_t = R_0^6 / R^6 + R_0^6$$

where E_t represents energy transfer efficiency, R is the distance between the fluorescent proteins, and R_0 is the donor–acceptor distance at which 50 % of the excitation energy is transferred whereas the remaining 50 % decays as non-radioactive or radioactive energy. This efficiency depends on the fluorescent partners used (Table 1).

4. The fluorescence lifetime of the donor molecule (quantum yield of the donor) must be long enough to allow energy transfer to the acceptor.

Several methods are used to determine and quantify FRET efficiency (*see* **Note 5**). To study receptor interactions in dynamic processes the most adequate FRET technique is based in the sensitized emission of the acceptor.

3.1.1 Sensitized Emission of the Acceptor

FRET efficiency can be determined in individual (fixed) cells using confocal microscopy or in living cell populations using a multilabel fluorescent plate reader with specific detectors. The method requires specific excitation of the donor fluorescent protein and use of specific light filters to determine donor and acceptor fluorescent emissions. Specific detectors must be used to collect the maximum peak of fluorescent emission for both donor and acceptor molecules.

As in other FRET methods, the donor emission spectrum must overlap the acceptor excitation spectrum. For many FRET partners, the requirement for spectral proximity can lead to strong fluorophore cross talk and cross-excitation processes that might alter quantitative analysis. To correct for detection of ratiometric signals and sensitized emission, a linear unmixing method is used that is based on the assumption that total detected signal (S) for each channel (λ) can be expressed as a linear combination of the contributing fluorophores (FluoX), according to the formula:

$$S(\lambda) = A_1 \times \mathrm{Fluo1}(\lambda) + A_2 \times \mathrm{Fluo2}(\lambda)$$

where An is the contribution of a specific fluorophore, and fluorophore concentration in the signal observed therefore determines their respective contribution to the total signal [50, 51]. This signal is redistributed into the specific fluorescence channels and can be analyzed quantitatively. To calculate fluorophore contributions, linear unmixing requires knowledge of reference values for samples that contain the fluorophores of interest separately. For successful separation of overlapping signals, the number of detection channels used and the number of fluorophores in the sample must be the same.

For highly efficient FRET partners such as CFP and YFP, which have very close overlapping signals, the FRET pair must be excited by a single excitation wavelength and FRET interactions resolved using linear unmixing (Fig. 1, example spectrum CFP-YFP, see FRET measurement). This is the best way to analyze the contribution of individual signals to the mixture.

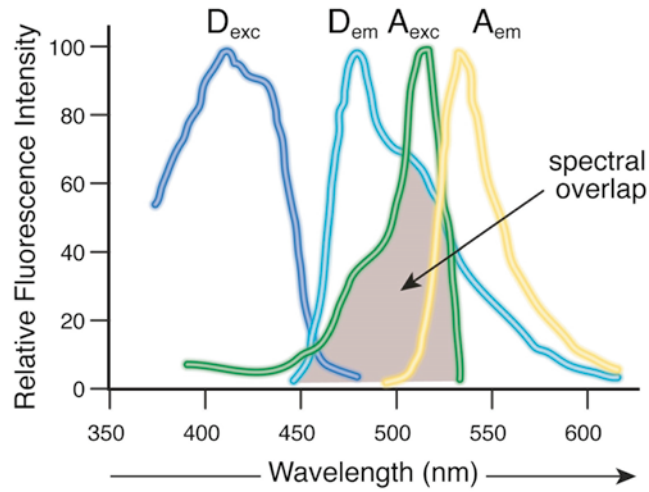

Fig. 1 Excitation and emission spectra of a CFP–YFP FRET pair. The scheme shows absorbance (exc) and emission (em) spectra of CFP (cyan fluorescent protein; donor; D) and YFP (yellow fluorescent protein; acceptor, A). Spectral overlap between CFP emission and YFP excitation (*shaded region*) is a prerequisite for FRET

3.1.2 FRET Saturation Curves by Sensitized Emission

1. Plate HEK293T cells (3.5×10^5 cells/well in 2 ml complete DMEM, using 6-well plates) and culture (24 h, 37 °C, 5 % CO_2).
2. To obtain FRET saturation curves, prepare two transfection mixtures: (*a*) mix 25 µl of 150 mM NaCl/µg of DNA and vortex (10 s); (*b*) at a 4:1 ratio, mix 150 mM NaCl and PEI (5.47 mM in nitrogen residues). Add mixture *b* to mixture *a* at a 1:1 ratio, vortex (10 s) and incubate (15–30 min, room temperature). Add the mixture (*a* + *b*) to the cells in 1 ml serum-free DMEM, incubate (4 h, 37 °C), and replace medium with complete DMEM (*see* **Note 6**).
3. At 48 h post-transfection, wash cells twice in HBSS supplemented with 0.1 % glucose and resuspend in this same buffer. Determine total protein concentration for each cell sample using a Bradford assay kit. Pipette Cell suspensions (20 µg protein/100 µl) into black 96-well microplates and read in a multilabel fluorescent plate reader equipped with a high-energy xenon flash lamp, a short-wavelength filter (8 nm bandwidth, 405 nm) and a long-wavelength emission filter (10 nm bandwidth, 486 nm for CFP channel and 10 nm bandwidth, 530 for YFP channel) (*see* **Note 7**). To determine the spectral signature, HEK293T cells are transiently transfected with the chemokine receptor coupled to CFP or to YFP separately. The contributions of CFP and YFP alone are measured in each detection channel and normalized to the sum of the signal obtained in both channels. Analyze the spectral signatures of CFP or YFP fused to chemokine receptors and check variability

(it must not vary significantly ($p > 0.05$)) from the signatures determined for each fluorescent protein alone. For FRET quantitation and receptor-YFP expression quantitation in FRET saturation curves, the spectral signature is taken into account for linear unmixing in order to separate the two emission spectra. To determine the fluorescence emitted by each fluorophore in FRET experiments, apply the following formulas:

$$\mathrm{CFP} = S / (1 + 1 / R) \text{ and } \mathrm{YFP} = S / 1 + R$$

where

$$S = \mathrm{ChCFP} + \mathrm{ChYFP},$$

$$R = (\mathrm{YFP}_{530}Q \quad \mathrm{YFP}_{486}) / (\mathrm{CFP}_{486} - \mathrm{CFP}_{530}Q), \text{ and}$$

$$Q = \mathrm{ChCFP} / \mathrm{ChYFP}$$

ChCFP and ChYFP represent the signal detected for CFP in the 486 nm and 530 nm detection channels (Ch), respectively; CFP_{486}, CFP_{530}, YFP_{530}, and YFP_{486} are the normalized contributions of CFP and YFP to 486 and 530 nm channels, as determined from their spectral signatures.

4. Sensitized emission FREt allows measurement of the energy transferred relative to the acceptor/donor ratio to generate FRET saturation curves. The curves show FRET efficiency as a function of the acceptor–donor ratio and are characterized by two important parameters; FRET_{max}, is the (asymptotic) maximum of the curve and FRET_{50} corresponds to the acceptor–donor ratio that yields half FRET_{max} efficiency (only when energy transfer reaches saturation and the curve is hyperbolic). FRET_{max} is associated with the number of receptor complexes formed and/or changes in complex conformation, and FRET_{50} allows estimation of the apparent affinity between the two partners that form the complex [52, 53]. These two parameters are deduced from data analysis using a nonlinear regression equation applied to a single binding site model (based on Michaelis–Menten model, Fig. 2) (*see* **Note 8**).

3.2 BRET

The BRET technique is based on non-radiative energy transfer between a bioluminescent donor (usually *Renilla* luciferase (Luc)) and a fluorophore acceptor. Like FRET, this method requires the generation of fusion proteins for donors between the receptor and luciferase (Luc) and for acceptors fusion between receptor and YFP, CFP, or GFP[2]. When Luc is present, it oxidizes its substrate (coelenterazine or DeepBlueC) and triggers photons release. Close proximity (10 nm) of an appropriate fluorophore ensures its excitation; that is, electron movement to a higher energetic state and thus, photon emission of longer wavelengths (*see* **Note 9**).

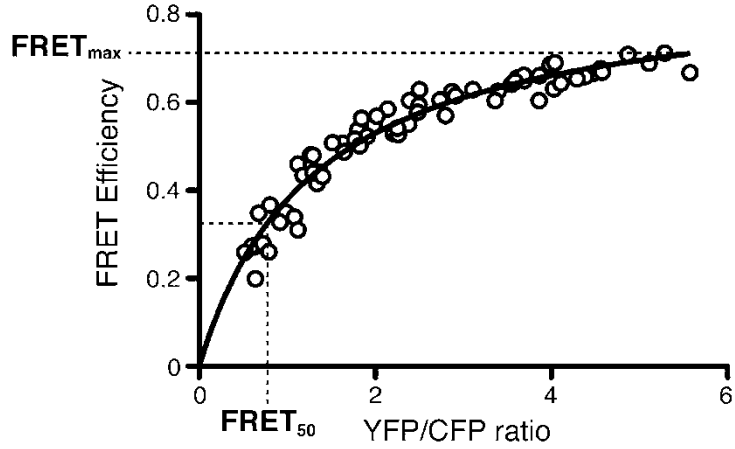

Fig. 2 FRET saturation curve generated by the sensitized emission method. A representative FRET saturation curve for a chemokine receptor pair. The curve reaches FRETmax (maximum FRET efficiency detected) and is hyperbolic. $FRET_{50}$ indicates the FRET efficiency value that corresponds to the acceptor–donor ratio (YFP–CFP ratio) that yields half FRETmax

3.2.1 BRET Titration Assays

1. Plate HEK293T cells (3.5×10^5 cells/well in 2 ml complete DMEM, using 6-well plates) and culture (24 h, 37 °C, 5 % CO_2).
2. Cotransfect the cells using the PEI protocol (*see* Subheading 3.1.1 above) with a constant amount of donor (Luc-fused chemokine receptor) and increasing amounts of acceptor protein (YFP-, CFP-, or GFP[2]-fused chemokine receptor, depending on the luciferase substrate; see above) (*see* **Note 10**).
3. At 48 h post-transfection, wash cells twice in HBSS supplemented with 0.1 % glucose and resuspend cells in this buffer. Using a Bradford assay, determine total protein concentration in each well.
4. Quantify the fluorescent protein (20 μg) using a multilabel plate reader equipped with a high-energy xenon flash lamp (for CFP or GFP[2] acceptor, 8 nm bandwidth excitation filter at 405 nm; for YFP, 10 nm bandwidth excitation filter at 510 nm). Receptor fluorescence expression is determined as fluorescence of the sample minus the fluorescence of cells that express donor alone. For BRET[2] and BRET[1] measurements, the equivalent of 20 μg cell suspension is distributed in 96-well microplates, followed by 5 μM DeepBlueC (for BRET[2]) or coelenterazine H (for BRET[1]). For BRET[2] experiments, signals are obtained immediately (30 s) after DeepBlueC addition using the multilabel plate reader, which allows integration of signals detected in the short- (8 nm bandwidth, 405 nm) and the long-wavelength filters (10 nm bandwidth, 486 nm). For BRET[1], readings are collected 1 min after coelenterazine H addition, as the plate

reader allows integration of signals detected in the short- (10 nm bandwidth, 510 nm) and long-wavelength filters (10 nm bandwidth, 530 nm). Receptor-Luc luminescence signals should be acquired 10 min after coelenterazine H (5 μM) addition. BRET efficiency ($BRET_{eff}$) is defined as:

$$BRET_{eff} = [(\text{long wavelength emission}) / (\text{short wavelength emission})] - C_f$$

where C_f is [(long wavelength emission)/(short wavelength emission)] for the Luc construct expressed alone in the same experiment (control).

5. Statistical analysis (*see* **Note 5** and Subheading 3.1.2 above).

3.3 Bimolecular Fluorescence Complementation (BiFC)

Bimolecular fluorescence complementation (BiFC) technology enables simple, direct visualization of protein–protein interactions in living cells [54–56]. The BiFC assay uses receptors fused to two fluorescent protein fragments that are nonfluorescent individually; fluorescence is recovered only when both fragments interact, that is, when the accompanying receptor form complexes. The approach can be used for analysis of interactions between many types of proteins and does not require information about the structures of the interaction partners (*see* **Note 11**).

Like FRET and BRET, BiFC requires fusion of the fluorescent protein fragments to chemokine receptors, as well as testing that neither protein expression nor receptor function is modified by the fluorescent fragments (*see* **Notes 12** and **13**).

3.3.1 BiFC Measurement

1. Plate HEK293T cells 24 h before transfection (3.5×10^5 cells/2 ml, in 6-well plates) and cultured (37 °C, 5 % CO_2).
2. Cotransfect using PEI or JetPei methods (according to manufacturer's protocol), with chemokine receptors fused to the nonfluorescent fragments at a 1:1 ratio (i.e., 0.7 μg CXCR4-nYFP + 0.7 μg CXCR4-cYFP) and culture (48 h, 37 °C, 5 % CO_2).
3. Wash cells with HBSS supplemented with 0.1 % glucose and resuspend in the same buffer. Determine the protein concentration in the cell pool using a Bradford assay kit (Bio-Rad).
4. Pipette cells into black 96-well plates, at 20 μg of protein in 100 μl (0.2 μg/μl) per well.
5. Quantify the fluorescent protein using a multilabel plate reader equipped with a high-energy xenon flash lamp (for YFP, 10 nm bandwidth excitation filter at 510 nm and 10 nm bandwidth emission filter at 530 nm).

3.4 BRET-BiFC

BRET-BiFC allows identification of heterotrimeric complexes in living cells. This method combines BRET and BiFC techniques sequentially. It is thus necessary take into account all controls and considerations described in Subheadings 2 and 3. In BRET-BiFC,

the donor is a Luc-fused chemokine receptor or protein and the acceptor is formed by interaction of the two nonfluorescent fragments fused to the chemokine receptors of interest.

1. Plate HEK293T cells (3.5×10^5 cells/well in 2 ml complete DMEM, use 6-well plates) and culture (24 h, 37 °C, 5 % CO_2).
2. Using the PEI method (*see* Subheading 3.1.2, **step 2** above), cotransfect cells with a constant amount of donor (Luc-fused chemokine receptor) and increasing amounts of a mixture of acceptor proteins at a 1:1 ratio (i.e., nYFP- and cYFP-fused chemokine receptors) (*see* **Note 14**).
3. At 48 h post-transfection, wash cells twice in HBSS supplemented with 0.1 % glucose and resuspend the pellet in the same buffer. Determine protein concentration for the cell pool using a Bradford assay kit.
4. Quantify the fluorescent protein in samples containing 20 μg protein, using a multilabel plate reader equipped with a high-energy xenon flash lamp (for YFP, 10 nm bandwidth excitation filter at 510 nm). Expression of the fluorescent protein-fused receptor is determined as fluorescence of the sample minus fluorescence of cells expressing donor-Luc alone. Distribute the cell suspension (20 μg/well) in 96-well microplates (Corning 3912, flat-bottom white plates). Add coelenterazine H (for BRET[1], 5 μM/well; PJK GmbH) and read 1 min later in the plate reader, which allows integration of signals detected in the short- (10 nm bandwidth, 510 nm) and long-wavelength filters (10 nm bandwidth, 530 nm). Receptor-Luc luminescence signals are acquired 10 min after coelenterazine H addition. BRET-BiFC efficiency is calculated using the same formula given for BRET efficiency in Subheading 3.2.1 above.

   In each BRET-BiFC titration curve, the relative amount of acceptor is given by the ratio between acceptor (YFP) formed by the two nonfluorescent proteins and the luciferase activity of the donor (Luc).
5. Statistical analysis as in Subheading 3.1.2 above (*see* **Note 5**).

3.5 Sequential BRET-FRET (SRET)

The SRET method allows detection of complexes of three proteins in living cells. There are several possible combinations depending on the donor and acceptor fusion proteins (Fig. 3).

SRET[1] combines BRET[1] and FRET. The first donor protein is a Luc-fused chemokine receptor. The first acceptor protein is YFP, which is then used as a second donor to excite the next acceptor, a chemokine receptor fused to dsRed, which is the signal detected. This method uses coelenterazine H as a Luc substrate.

SRET[2] combines BRET[2] and FRET. The Luc-fused chemokine receptor is the first donor (using DeepBlueC as a specific Luc substrate). T CFP- or GFP[2]-fused receptor is then excited and its

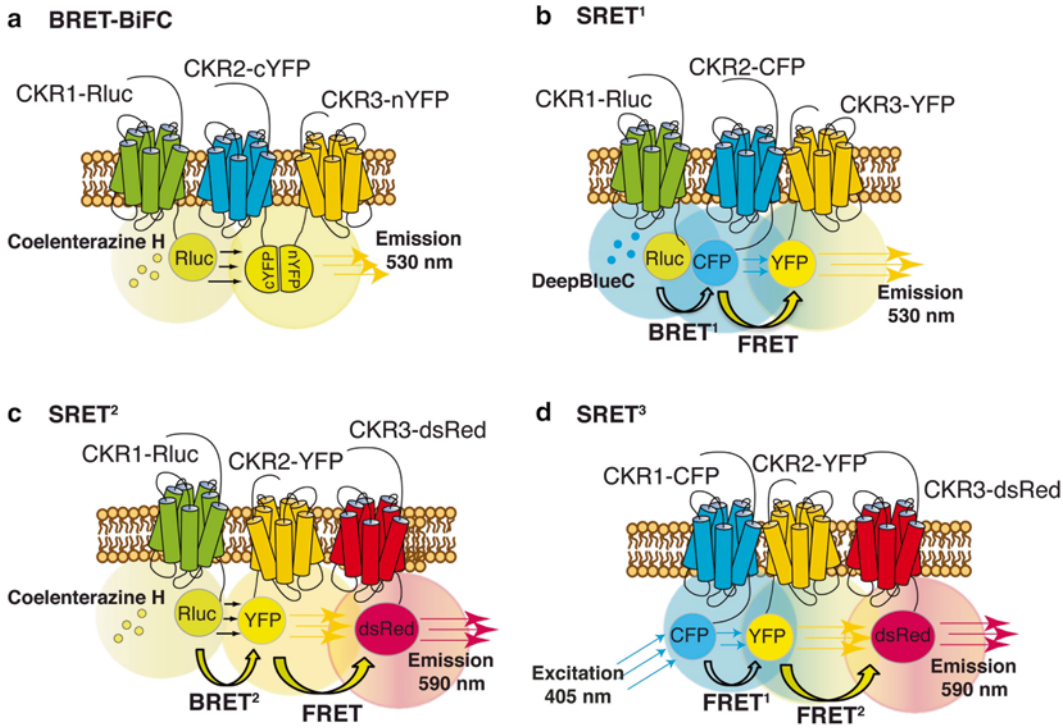

Fig. 3 Scheme of BRET-BiFC, SRET[1], SRET[2], and SRET[3] techniques. (**a**) BRET-BiFC for the chemokine receptors CKR1, CKR2, and CKR3 fused to Rluc, cYFP, and nYFP, respectively. Following interaction between chemokine receptors CKR2 and CKR3 (*colored halos*), YFP is reconstituted and is susceptible to excitation by Rluc activated by its substrate, coelenterazine H (*yellow dots*). EYFP emission is detected at 530 nm. (**b**) SRET[1] for the chemokine receptors CKR1, CKR2, and CKR3 fused to Rluc, CFP, and YFP, respectively. Due to activation by its substrate DeepBlueC (*blue dots*), Rluc excites CFP (BRET), which in turn excites YFP (FRET) that is detected at 530 nm. (**c**) In SRET[2], initial BRET between Luc and YFP triggered by coelenterazine H (*yellow dots*) excites dsRed, the last acceptor fluorescence protein, which then emits light at 590 nm. (**d**) SRET[3] is a FRET[1] and FRET[2] sequence. Due to the interaction between CFP, YFP, and dsRed fused to a chemokine receptor (CKR1, CKR2, CKR3, respectively), CFP excitation (at 405 nm) triggers dsRed light emission at 590 nm

emission energy (BRET[2]) excites the YFP-fused receptor, which is then the last SRET acceptor.

SRET[3] combines two sequential FRET methods. The donor protein is the CFP- or GFP[2]-fused chemokine, the first acceptor/second donor is the YFP-fused receptor which excites the last acceptor, which is the dsRed-fused receptor.

Here we describe in detail the SRET[2] method, which can easily be adapted for SRET[1] or SRET[3] using the detection filters for each specific fluorophore and the appropriate Luc substrate in the case of SRET[1].

1. Plate HEK293T cells (3.5×10^5 cells/well in 2 ml complete DMEM, use 6-well plates) and culture (24 h, 37 °C, 5 % CO_2).
2. Using the PEI method (Subheading 3.1.2, **step 2** above), cotransfect the cells with a constant amount of Luc-fused

receptor and increasing amounts of receptor fused to acceptors (CFP or GFP^2 and YFP at 1:1 ratio); culture (48 h, 37 °C, 5 % CO_2).

3. Wash cells with HBSS supplemented with 0.1 % glucose and resuspend the pellet in the same buffer. Total protein concentration is determined for the cell pool using a Bradford assay kit (Bio-Rad).
4. Use aliquots of transfected cells (20 μg protein/100 μl in a 96-well microplate) to perform three experiments in parallel.
5. In the first experiment, quantify FRET efficiency for the FRET pairs used (CFP or GFP^2 and YFP) and the amount of acceptor protein–YFP at each ratio. Distribute cells (20 μg) in black 96-well microplates and read in a multilabel plate reader equipped with a high-energy xenon flash lamp, using an excitation filter at 405 ± 8 nm and 10 nm bandwidth emission filters corresponding to 530 nm (channel 1) and 486 nm (channel 2). As in FRET, separate the relative contribution of fluorophores to each detection channel for linear unmixing. Then measure the contribution of CFP or GFP^2 and YFP proteins alone to the two detection channels and normalize to the sum of the total signal obtained in the two detection channels. Quantify the total amount of receptor-YFP at each ratio in the same equipment using a 510 ± 10 nm excitation filter at and a 530 ± 10 nm emission filter.
6. In the second experiment, quantify the receptor-Luc expression by determining its luminescence. Pipette the cells (20 μg) into 96-well microplates (white-bottomed white plates), add the substrate (5 μM coelenterazine H); after 10 min, detect luminescence in a multilabel plate reader.
7. For SRET[1] evaluation in the third experiment, distribute cells (20 μg) in 96-well microplates (white-bottomed white plates) and add 5 μM DeepBlueC as Luc substrate; after 30 s, collect the SRET signal using a multilabel plate reader with detection filters for short (486 nm) and long wavelengths (530 nm).
8. By analogy with BRET, net SRET is defined as:

$$\text{netSRET} = ((\text{long wavelength emission}) / (\text{short wavelength emission})) - C_f$$

where

$$C_f = ((\text{long wavelength emission}) / (\text{short wavelength emission})$$

for cells expressing the receptor-Luc, receptor-CFP or -GFP^2 separately. SRET is only detected if all receptors interact and the corresponding pairs (Luc/CFP or Luc/GFP^2 and CFP/YFP or GFP^2/YFP or Luc/YFP) are located at <10 nm distance.

9. For statistical analysis, *see* Subheading 3.1.2 above and **Note 5**.

4 Notes

1. Any other cell line with high transfection efficiency for the receptors of interest can be employed. In this case the transfection method should be optimized to these cell lines. Take into account that most cell lines can express endogenously chemokine receptors (most frequently CXCR4) that may alter chemokine oligomers.
2. Several plasmids are commercially available to fuse fluorescent proteins to a receptor (Clontech).
3. For chemokine receptors and to avoid interference with ligand binding it is best to fuse fluorescent proteins to the C-terminal end of the receptor.
4. All the techniques described in this chapter require fusion of chemokine receptors to fluorescent (FRET) or luminescent proteins (BRET), or N- or C-terminal fragments of fluorescent proteins (BiFC). Insertion of a fluorescent probe in the C-terminal region of the receptor involves eliminating the receptor stop codon, whereas N-terminal insertion requires elimination of the fluorescent protein stop codon. Transfected cells should therefore be analyzed for receptor expression and function.

   The constructs are obtained using standard molecular biology techniques in commercially available vectors that bear the luminescent or fluorescent proteins (Clontech). In the case of BiFC, the fluorescent protein used must be cut into N- and C-terminal fragments, which must then be included in separate expression vectors (i.e., pcDNA3.1; *see* Table 2). Insertion of these fragments in-frame with the chemokine receptor C-terminal region requires elimination of the receptor stop codon. Transfected cells with these chimeric proteins should be tested for receptor expression and function.

   Several experiments are needed to test whether the chimeric proteins maintain expression and function. Using flow cytometry, stain the chemokine receptors expressed at the cell surface with specific antibodies. Chemokine receptor function is usually tested using calcium mobilization assays or migration in transwells. The chemokine receptors fused to fluorescent/luminescent proteins must behave similarly to the wild type receptor.
5. Methods used to determine and quantify FRET efficiency include:
   (a) *Donor quenching or acceptor photobleaching* is a method based on quenching donor fluorescence. As some donor photons excite the acceptor, a decrease is detected in donor emission energy. After acceptor photobleaching, increased donor light emission is detected. Due to cell damage caused by the extended laser exposure needed to photobleach the acceptor, this method cannot be used in live cells.

(b) For *sensitized emission of the acceptor*, the acceptor signal is quantitated after donor excitation. This method is useful to determine FRET in dynamic processes in the cell, such as the consequences of ligand stimulation, the effects triggered by other proteins coexpressed on cell surface, and so on.

(c) *Fluorescence lifetime imaging microscopy (FLIM)* is a method based on measurement of a constant parameter of each fluorescent protein in each experimental condition, termed lifetime. Lifetime is the duration of the excited state of a fluorophore before returning to its ground state. This technique allows spatial resolution of biochemical processes. The fluorescence lifetime of a donor molecule decreases in FRET conditions independently of fluorescent protein concentrations and of excitation intensities.

6. The cells must be transiently cotransfected with a constant amount of donor (chemokine receptor fused to the donor fluorophore, CFP) and increasing amounts of acceptor protein (chemokine receptor fused to the acceptor fluorophore, YFP) using the polyethylenimine method (PEI).
7. Gain settings must be identical for all experiments to maintain a constant relative contribution of each fluorophore to the detection channels for spectral imaging and linear unmixing.
8. Statistical analysis is needed to reduce experimental variability (at least five replications of the saturation curves are usually generated), and will finally determine the homogeneous curves. We currently use three distinct statistical methods (bootstrap, F test, and Akaike information criterion (AIC)), which usually lead to similar conclusions [57]. For example, we can determine the conformational changes in dimers promoted by a given ligand ("the treatment"). Curves for untreated and ligand-treated groups are naturally paired when dimerization is evaluated in the same group of cells before and after "treatment." To determine which model best fits the data for pairs of saturation curves, we use the AIC method corrected for small size samples ($n \leq 10$), in which the null hypothesis is one curve for all data sets (before and after "treatment") and the alternative hypothesis is the existence of different curves for each data set. If the majority of the AICc difference (Δ) is positive, the preferred model is a distinct curve for all data sets, whereas if Δ is negative, the preferred model is a single curve for all data sets [28]. When the number of individual determinations (n) in each curve is >10 observations, a *t*-test can be used to compare the components of each pair [58–60]. When the p value is <0.05, we can conclude that the changes observed after a specific treatment are statistically significant.

9. Distinct luciferase substrates can be chosen depending on the acceptor fluorophore. Requirements for energy transfer in BRET are the same that those for FRET (*see* Subheading 3.1 above). The most used luciferase substrates are coelenterazine, used in BRET[1] assays, whose maximal emission is at 515 nm and which is used in combination with YFP as acceptor. DeepBlueC, used in BRET[2] assays, is an analogue of the natural luciferase substrate with maximal emission wavelength at 410 nm; it is used in combination with CFP or GFP[2], which emit at 485 nm and 515 nm respectively, yielding a spectral separation of >100 nm.
10. The cells must also be transfected separately with donor and acceptor. Use untransfected HEK293T cells as a background control for each experiment.
11. One advantage of this technique is that the complex formed has strong intrinsic fluorescence, which allows direct visualization of the protein interaction without exogenous agents. This avoids disturbance of the cells, but also is a clear disadvantage, as the user must know that there is a delay between the time needed by the proteins to interact and the time required for the reconstituted complex to become fluorescent [54].
12. Flexible linker sequences are recommended, to allow maximal mobility of the nonfluorescent fragments after complex formation.
13. To determine BiFC specificity, many controls are included in each experiment, such as nonfluorescent fragment-fused receptors with point mutations in the interaction interface that impede reconstitution of the complete protein [55, 61]. Control proteins with the same cell expression pattern as the chemokine receptors should be included.
14. Controls include cells transfected with the receptor-Luc construct alone and with receptors fused to the acceptor fragments. In addition, untransfected HEK293T cells are needed to determine the background.

Acknowledgments

We specially thank the present and former members of the DIO chemokine group who contributed to some of the work described in this review. We also thank C. Bastos and C. Mark for secretarial support and editorial assistance, respectively. This work was partially supported by grants from the Spanish Ministry of Economy and Competitiveness (SAF-2011-27270), the RETICS Program (RD 12/0009/009 RIER) and the Madrid regional government (S2010/BMD-2350; RAPHYME).

References

1. Griffith JW, Sokol CL, Luster AD (2014) Chemokines and chemokine receptors: positioning cells for host defense and immunity. Annu Rev Immunol 32:659–702
2. Bachelerie F, Ben-Baruch A, Burkhardt AM et al (2013) International Union of Basic and Clinical Pharmacology. [corrected]. LXXXIX. Update on the extended family of chemokine receptors and introducing a new nomenclature for atypical chemokine receptors. Pharmacol Rev 66:1–79
3. Baggiolini M (1998) Chemokines and leukocyte traffic. Nature 392:565–568
4. Rossi D, Zlotnik A (2000) The biology of chemokines and their receptors. Annu Rev Immunol 18:217–242
5. Mackay CR (2001) Chemokines: immunology's high impact factors. Nat Immunol 2:95–101
6. Balkwill F (2004) Cancer and the chemokine network. Nat Rev Cancer 4:540–550
7. Baggiolini M, Dahinden CA (1994) CC chemokines in allergic inflammation. Immunol Today 15:127–133
8. Belperio JA, Keane MP, Arenberg DA et al (2000) CXC chemokines in angiogenesis. J Leukoc Biol 68:1–8
9. Gerard C, Rollins BJ (2001) Chemokines and disease. Nat Immunol 2:108–115
10. Godessart N, Kunkel SL (2001) Chemokines in autoimmune disease. Curr Opin Immunol 13:670–675
11. Proudfoot AE (2002) Chemokine receptors: multifaceted therapeutic targets. Nat Rev Immunol 2:106–115
12. Proudfoot AE, Handel TM, Johnson Z et al (2003) Glycosaminoglycan binding and oligomerization are essential for the in vivo activity of certain chemokines. Proc Natl Acad Sci U S A 100:1885–1890
13. Jansma A, Handel TM, Hamel DJ (2009) Chapter 2. Homo- and hetero-oligomerization of chemokines. Methods Enzymol 461:31–50
14. Hamel DJ, Sielaff I, Proudfoot AE, Handel TM (2009) Chapter 4. Interactions of chemokines with glycosaminoglycans. Methods Enzymol 461:71–102
15. Salanga CL, Handel TM (2011) Chemokine oligomerization and interactions with receptors and glycosaminoglycans: the role of structural dynamics in function. Exp Cell Res 317:590–601
16. Alcami A (2003) Viral mimicry of cytokines, chemokines and their receptors. Nat Rev Immunol 3:36–50
17. Seet BT, McFadden G (2002) Viral chemokine-binding proteins. J Leukoc Biol 72:24–34
18. Murphy PM (2001) Viral exploitation and subversion of the immune system through chemokine mimicry. Nat Immunol 2:116–122
19. De Paula VS, Gomes NS, Lima LG et al (2013) Structural basis for the interaction of human β-defensin 6 and its putative chemokine receptor CCR2 and breast cancer microvesicles. J Mol Biol 425:4479–4495
20. Chabre M, Deterre P, Antonny B (2009) The apparent cooperativity of some GPCRs does not necessarily imply dimerization. Trends Pharmacol Sci 30:182–187
21. Hernanz-Falcón P, Rodríguez-Frade JM, Serrano A et al (2004) Identification of amino acid residues crucial for chemokine receptor dimerization. Nat Immunol 5:216–223
22. Rodríguez-Frade JM, Mellado M, Martínez-A C (2001) Chemokine receptor dimerization: two are better than one. Trends Immunol 22:612–617
23. Rodríguez-Frade JM, Vila-Coro AJ, de Ana AM et al (1999) The chemokine monocyte chemoattractant protein-1 induces functional responses through dimerization of its receptor CCR2. Proc Natl Acad Sci U S A 96: 3628–3633
24. Thelen M, Muñoz LM, Rodríguez-Frade JM, Mellado M (2010) Chemokine receptor oligomerization: functional considerations. Curr Opin Pharmacol 10:38–43
25. Wu B, Chien EY, Mol CD et al (2010) Structures of the CXCR4 chemokine GPCR with small-molecule and cyclic peptide antagonists. Science 330:1066–1071
26. Barroso R, Martínez Muñoz L, Barrondo S et al (2012) EBI2 regulates CXCL13-mediated responses by heterodimerization with CXCR5. FASEB J 26:4841–4854
27. Pello OM, Martínez-Muñoz L, Parrillas V et al (2008) Ligand stabilization of CXCR4/delta-opioid receptor heterodimers reveals a mechanism for immune response regulation. Eur J Immunol 38:537–549
28. Martínez-Muñoz L, Barroso R, Dyrhaug SY et al (2014) CCR5/CD4/CXCR4 oligomerization prevents HIV-1 gp120IIIB binding to the cell surface. Proc Natl Acad Sci U S A 111:E1960–E1969
29. Iizumi M, Bandyopadhyay S, Watabe K (2007) Interaction of Duffy antigen receptor for chemokines and KAI1: a critical step in metastasis suppression. Cancer Res 67:1411–1414

30. Kumar A, Humphreys TD, Kremer KN et al (2006) CXCR4 physically associates with the T cell receptor to signal in T cells. Immunity 25:213–224
31. Herrera C, Morimoto C, Blanco J et al (2001) Comodulation of CXCR4 and CD26 in human lymphocytes. J Biol Chem 276:19532–19539
32. Yoshida T, Ebina H, Koyanagi Y (2009) N-linked glycan-dependent interaction of CD63 with CXCR4 at the Golgi apparatus induces downregulation of CXCR4. Microbiol Immunol 53:629–635
33. Mellado M, Rodríguez-Frade JM, Vila-Coro AJ et al (2001) Chemokine receptor homo- or heterodimerization activates distinct signaling pathways. EMBO J 20:2497–2507
34. Rozenfeld R, Devi LA (2010) Receptor heteromerization and drug discovery. Trends Pharmacol Sci 31:124–130
35. Mellado M, Rodríguez-Frade JM, Vila-Coro AJ et al (1999) Chemokine control of HIV-1 infection. Nature 400:723–724
36. Molon B, Gri G, Bettella M et al (2005) T cell costimulation by chemokine receptors. Nat Immunol 6:465–471
37. Chen C, Li J, Bot G et al (2004) Heterodimerization and cross-desensitization between the mu-opioid receptor and the chemokine CCR5 receptor. Eur J Pharmacol 483:175–186
38. Szabo I, Wetzel MA, Zhang N et al (2003) Selective inactivation of CCR5 and decreased infectivity of R5 HIV-1 strains mediated by opioid-induced heterologous desensitization. J Leukoc Biol 74:1074–1082
39. Rodríguez-Frade JM, Vila-Coro AJ, Martín A et al (1999) Similarities and differences in RANTES- and (AOP)-RANTES-triggered signals: implications for chemotaxis. J Cell Biol 144:755–765
40. Percherancier Y, Berchiche YA, Slight I et al (2005) Bioluminescence resonance energy transfer reveals ligand-induced conformational changes in CXCR4 homo- and heterodimers. J Biol Chem 280:9895–9903
41. Wilson S, Wilkinson G, Milligan G (2005) The CXCR1 and CXCR2 receptors form constitutive homo- and heterodimers selectively and with equal apparent affinities. J Biol Chem 280:28663–28674
42. Harrison C, van der Graaf PH (2006) Current methods used to investigate G protein coupled receptor oligomerisation. J Pharmacol Toxicol Methods 54:26–35
43. Pfleger KD, Eidne KA (2006) Illuminating insights into protein-protein interactions using bioluminescence resonance energy transfer (BRET). Nat Methods 3:165–174
44. Cardullo RA (2007) Theoretical principles and practical considerations for fluorescence resonance energy transfer microscopy. Methods Cell Biol 81:479–494
45. Boute N, Jockers R, Issad T (2002) The use of resonance energy transfer in high-throughput screening: BRET versus FRET. Trends Pharmacol Sci 23:351–354
46. Coulon V, Audet M, Homburger V et al (2008) Subcellular imaging of dynamic protein interactions by bioluminescence resonance energy transfer. Biophys J 94:1001–1009
47. Pfleger KD, Seeber RM, Eidne KA (2006) Bioluminescence resonance energy transfer (BRET) for the real-time detection of protein-protein interactions. Nat Protoc 1:337–345
48. El-Asmar L, Springael JY, Ballet S et al (2005) Evidence for negative binding cooperativity within CCR5-CCR2b heterodimers. Mol Pharmacol 67:460–469
49. Marullo S, Bouvier M (2007) Resonance energy transfer approaches in molecular pharmacology and beyond. Trends Pharmacol Sci 28:362–365
50. Dickinson ME, Bearman G, Tille S et al (2001) Multi-spectral imaging and linear unmixing add a whole new dimension to laser scanning fluorescence microscopy. Biotechniques 31:1272, 1274–1276, 1278
51. Zimmermann T, Rietdorf J, Girod A et al (2002) Spectral imaging and linear un-mixing enables improved FRET efficiency with a novel GFP2-YFP FRET pair. FEBS Lett 531: 245–249
52. Mercier JF, Salahpour A, Angers S et al (2002) Quantitative assessment of beta 1- and beta 2-adrenergic receptor homo- and heterodimerization by bioluminescence resonance energy transfer. J Biol Chem 277:44925–44931
53. Fuxe K, Ferré S, Canals M et al (2005) Adenosine A2A and dopamine D2 heteromeric receptor complexes and their function. J Mol Neurosci 26:209–220
54. Hu CD, Chinenov Y, Kerppola TK (2002) Visualization of interactions among bZIP and Rel family proteins in living cells using bimolecular fluorescence complementation. Mol Cell 9:789–798
55. Hu CD, Kerppola TK (2003) Simultaneous visualization of multiple protein interactions in living cells using multicolor fluorescence complementation analysis. Nat Biotechnol 21: 539–545

56. Kerppola TK (2006) Visualization of molecular interactions by fluorescence complementation. Nat Rev Mol Cell Biol 7:449–456
57. Baíllo A, Martínez-Muñoz L, Mellado M (2013) Homogeneity tests for Michaelis-Menten curves with application to fluorescence resonance energy transfer data. J Biol Syst 21:1350017
58. Levoye A, Balabanian K, Baleux F et al (2009) CXCR7 heterodimerizes with CXCR4 and regulates CXCL12-mediated G protein signaling. Blood 113:6085–6093
59. Martínez Muñoz L, Lucas P, Navarro G et al (2009) Dynamic regulation of CXCR1 and CXCR2 homo- and heterodimers. J Immunol 183:7337–7346
60. Motulsky H, Christopoulos A (2004) Fitting models to biological data using linear and nonlinear regression: a practical guide to curve fitting. Oxford University Press, New York
61. Grinberg AV, Hu CD, Kerppola TK (2004) Visualization of Myc/Max/Mad family dimers and the competition for dimerization in living cells. Mol Cell Biol 24:4294–4308